

Cite this: DOI: 10.1039/c0xx00000x

www.rsc.org/xxxxxx

PERSPECTIVE

# Photoinduced electron tunneling between randomly dispersed donors and acceptors in frozen glasses and other rigid matrices

Oliver S. Wenger,\*<sup>a</sup>*Received (in XXX, XXX) Xth XXXXXXXXX 20XX, Accepted Xth XXXXXXXXX 20XX*

DOI: 10.1039/b000000x

In fluid solution un-tethered donors and acceptors can diffuse freely, and consequently the donor-acceptor distance is usually not fixed on the timescale of an electron transfer event. When attempting to investigate the influence of driving-force changes or donor-acceptor distance variations on electron transfer rates this can be a problem. In rigid matrices diffusion is suppressed, and it becomes possible to investigate fixed-distance electron transfer. This method represents an attractive alternative to investigating rigid rod-like donor-bridge-acceptor molecules which have to be made in elaborate syntheses. This Perspective focuses specifically on the distance dependence of photoinduced electron transfer which occurs via tunneling of charge carriers through rigid matrices over distances between 1 and 33 Å. Some key aspects of the theoretical models commonly used for analyzing kinetic data of electron tunneling through rigid matrices are recapitulated. New findings from this rather mature field of research are emphasized.

Long-range electron transfer is an important process in chemistry, physics, and biology.<sup>1</sup> For example, biochemical redox reactions can occur at significant rates even when the two reaction partners are separated by more than 20 Å.<sup>2</sup> Photoinduced electron transfer is frequently investigated in fluid solution but for many applications it is desirable to understand the fundamentals of light-triggered charge transfer in rigid media. This is true for example for photoinduced electron transfer in composites of conducting polymers which are used in organic ("plastic") solar cells or in organic light-emitting diodes (OLEDs).<sup>3–5</sup>

One of the main reasons why chemists initially became interested in electron transfer between randomly dispersed donors and acceptors in rigid matrices is the fact that diffusion processes can make investigation of electron transfer kinetics difficult. While searching for the so-called inverted driving-force effect predicted by Marcus theory, it became evident that studying fixed-distance electron transfer is desirable.<sup>6</sup> One approach to ensure a fixed donor-acceptor distance on the timescale of an electron transfer event is to covalently link the reactants to one another.<sup>7, 8</sup> However, this approach can be synthetically tedious, and therefore immobilization of untethered donors and acceptors in rigid matrices represents an attractive alternative. In early studies involving rigid matrices the electron transfer events were triggered by pulse radiolysis,<sup>9–11</sup> and the focus was on elucidating the dependence of electron transfer rates on reaction free energy.<sup>12–15</sup> Over the years, light-induced electron transfer became more popular, and the focus shifted towards exploring the dependence of electron transfer rates on the distance between the donor and the acceptor.<sup>11, 16</sup> It is primarily the latter aspect which represents the focal point of the current Perspective, the earlier pulse radiolysis work is not reviewed here.

To the best of the author's knowledge, there has been no prior review on the subject of photoinduced electron tunneling between randomly dispersed donors and acceptors in glassy matrices; a related other review on the more general subject of electron transfer in the solid state dates from 1987.<sup>17</sup> The field of electron tunneling in glasses is very mature; much important work was performed well before 1980,<sup>1, 10, 18</sup> and the peak activity was reached in the 1980s. Between 1990 and 2000 this research area has been somewhat dormant but in more recent years it has experienced a revival. The current Perspective therefore seems timely, particularly in view of recent important insights gained regarding the analysis of time-dependent luminescence decay data,<sup>19</sup> electron tunneling through aqueous and organic glasses,<sup>20</sup> driving-force studies of electron transfer in ionic liquids,<sup>21, 22</sup> and in view of the importance of long-range electron transfer in polymers for plastic solar cells and OLEDs. Notably, recent studies of electron tunneling in glassy matrices have significantly advanced the general understanding of the distance dependence of long-range electron transfer, in particular with respect to the dependence of the electronic coupling between distant donors and acceptors on the intervening medium separating two reactants.<sup>23, 24</sup> As should be evident from the title and the abstract, the scope of this Perspective is restricted to systems in which both the electron donors and electron acceptors are randomly dispersed in glassy matrices and related rigid (and highly viscous) media. Photoinduced charge-separation in polymer blends or polymer heterojunctions (as investigated in the context of plastic solar cell research) is not reviewed here; reviews of this vast field of research are already available in the literature.<sup>3, 25</sup>

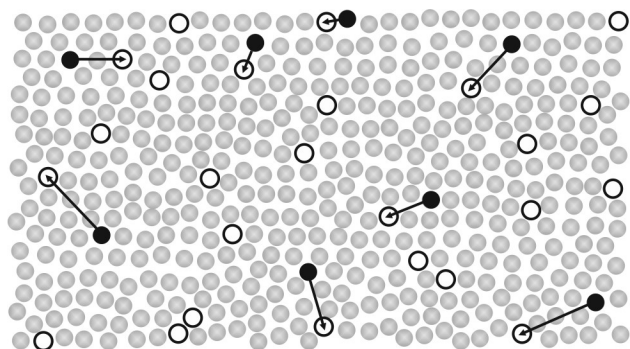


Figure 1. Illustration of photoinduced electron transfer between randomly dispersed donors and acceptors. Black filled circles: donors; grey circles: molecules of the rigid matrix; open circles: acceptors.

some conclusions.

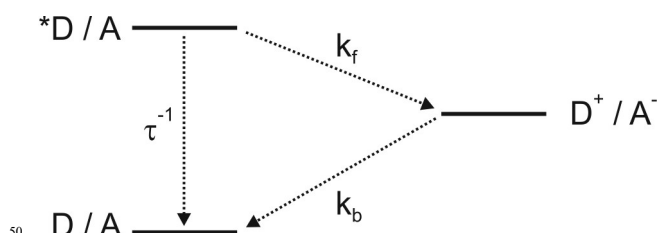


Figure 2. Energy level diagram illustrating photoinduced (forward) electron transfer from a neutral donor to a neutral acceptor, and thermal (back) electron transfer from reduced acceptor to oxidized donor.

## 2. Theoretical background

Under the assumption that the donor has only one photoactive excited state and the acceptor has only one accepting state the simple three-level diagram of Figure 2 provides an adequate description of the photoinduced electron transfer chemistry occurring between randomly dispersed donors (D) and acceptors (A) in a rigid matrix. After pulsed excitation, the photoactive state of D decays with an intrinsic lifetime ( $\tau$ ) governed by emission and nonradiative (multiphonon) relaxation processes. In presence of electron acceptors, electron transfer from the excited state of D to A becomes an alternative excited-state deactivation pathway, and this leads to a faster luminescence decay and a decrease of the time-integrated emission intensity. In a subsequent dark reaction  $D^+$  and  $A^-$  react back to the initial state. The rates of forward ( $k_f$ ) and backward electron transfer ( $k_b$ ) and their dependence on the D – A distance are usually of central interest in investigations of electron transfer in rigid matrices.<sup>2</sup>

Semiclassical theory describes electron transfer rates ( $k_{ET}$ ) as a product of a frequency prefactor, an electronic factor ( $H_{DA}$ ), and a nuclear factor.<sup>30</sup> The interplay of reaction free energy ( $\Delta G_{ET}^0$ ) and reorganization energy ( $\lambda$ ) in the nuclear factor defines the well-known Gaussian free energy dependence of electron transfer rates. Neither  $\Delta G_{ET}^0$  nor  $\lambda$  can be determined easily for D / A pairs in rigid matrices, but it is possible to obtain estimates based on  $\Delta G_{ET}^0$  and  $\lambda$  values that have been determined in fluid solution. For instance, the change from fluid solution (at 298 K) to a rigid 2-methyltetrahydrofuran glass (at 77 K) was found to lead to a decrease of  $\Delta G_{ET}^0$  for electron transfer between a photoexcited porphyrin and various benzoquinones by about 0.8 eV.<sup>31</sup> The influence of rigid media on  $\lambda$  can be similarly drastic.<sup>17, 28</sup> Outer-sphere reorganization is severely limited in rigid media; the static dielectric constant approaches the optical dielectric constant and the outer-sphere reorganization energy ( $\lambda_o$ ) can approach zero.

For a given D / A couple both  $\Delta G_{ET}^0$  and  $\lambda$  can vary as a function of D – A distance,<sup>32, 33</sup>  $H_{DA}$  is usually assumed to exhibit an exponential distance dependence as discussed below.<sup>34</sup> For non-driving-force optimized systems ( $-\Delta G_{ET}^0 \neq \lambda$ ) complicated distance dependences of  $k_{ET}$  can result.<sup>35</sup> Many of the glassy systems discussed in this review were investigated at 77 K, i. e., under experimental conditions at which very little thermal energy is available. Consequently, in the classical picture only electron transfers with small activation barriers are likely to be efficient, and many of these systems are therefore likely to be nearly

activationless ( $-\Delta G_{\text{ET}}^0 \approx \lambda$ ). The distance dependence of  $k_{\text{ET}}$  is then often assumed to be governed by the distance dependence of the electronic factor ( $H_{\text{DA}}^2$ ), and contributions from variations of  $\Delta G_{\text{ET}}^0$  and  $\lambda$  with increasing  $D - A$  distance are neglected.  $H_{\text{DA}}$  describes the electronic coupling between distant donors and acceptors through superexchange interactions and its magnitude decreases exponentially with increasing  $D - A$  distance.<sup>34</sup> The distance dependence of the forward and backward electron transfer rates can then be described as:

$$k_{\text{f}}(r) = k_{\text{f}}(R_0) \cdot \exp[-\beta_{\text{f}} \cdot (r - R_0)] \quad (1a)$$

$$k_{\text{b}}(r) = k_{\text{b}}(R_0) \cdot \exp[-\beta_{\text{b}} \cdot (r - R_0)] \quad (1b)$$

In these equations,  $R_0$  is the center-to-center donor-acceptor distance at van der Waals contact (commonly estimated by molecular modeling), and  $k_{\text{f}}(R_0)$  and  $k_{\text{b}}(R_0)$  are the rate constants for forward and backward electron transfer when donor and acceptor are in van der Waals contact. The  $\beta$  parameters are the so-called distance decay constants for photoinduced charge-separation ( $\beta_{\text{f}}$ ) and thermal charge-recombination ( $\beta_{\text{b}}$ ). Determination of these  $\beta$  values is a key goal of investigations of photoinduced electron transfer in rigid matrices, as they capture the efficiency of long-range electron transfer in a single number. For reference, the  $\beta$  parameter of vacuum has been calculated to 2.9 – 4.0 Å<sup>-1</sup>,<sup>36</sup> protein backbone typically yields  $\beta$ -values around 1.1 Å<sup>-1</sup>,<sup>37</sup> while some of the most efficient molecular wires exhibit  $\beta$ -values on the order of 0.1 Å<sup>-1</sup> or below.<sup>38</sup> However, it should be noted that the  $\beta$  parameter is clearly a property of a given combination of donor, acceptor, and intervening medium;<sup>39-41</sup> only to a crude approximation is it a bridge or intervening medium specific property.

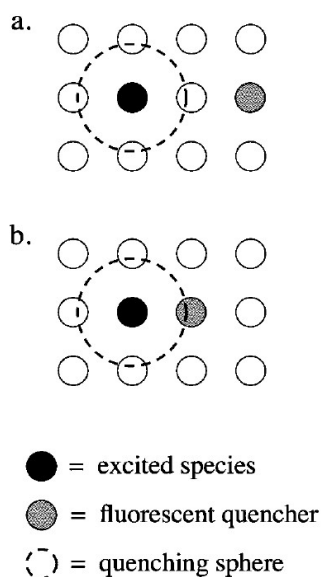


Figure 3. Illustration of the Perrin model: (a) quencher beyond the critical quenching radius ( $R_0$ ); (b) quencher within  $R_0$ . Reprinted with permission from ref. 42. Copyright 2008 American Chemical Society.

Most experimental studies of randomly dispersed donors and acceptors in rigid matrices have focused on the forward process in Figure 2 because it is easier to detect experimentally and

analyze theoretically than the backward reaction. The common experimental observable for forward electron transfer is the donor luminescence intensity.

Various theoretical models for analyzing time-dependent luminescence intensities ( $I(t)$ ) have been developed. The common starting point for these models is the radial pair distribution function (eq. 2) which describes the local density of molecules within a given radius ( $r$ ) around a central molecule in relation to the average density of molecules ( $\rho$ ).

$$g(r) = \frac{1}{4 \cdot \pi \cdot \rho \cdot r^2} \cdot \frac{dN}{dr} \quad (2)$$

In the following a few of the commonly used models will be briefly described. The idea is to give an overview of the methodology for data analysis, but for rigorous derivations of the individual mathematical equations the reader is referred to the original references cited in the appropriate places below. A review comparing different theoretical methods has already been published.<sup>43</sup>

The Perrin model (also called the sphere of action model or capture volume model) defines a critical quenching radius ( $R_0$ ) at which the rate for photoinduced electron transfer equals the inherent excited-state decay rate, i. e.,  $k_{\text{f}}(R_0) = \tau^{-1}$ . At  $D - A$  distances  $R \ll R_0$  the emission is completely quenched, but when  $R \gg R_0$  the luminescence remains unperturbed (Figure 3). Assuming the distribution of  $D$  and  $A$  is random,  $R_0$  is a simple function of the critical quencher concentration  $[A]_{\text{q}}$ :

$$R_0 = (4/3 \cdot \pi \cdot [A]_{\text{q}})^{-1/3} \quad (3)$$

$[A]_{\text{q}}$  is the concentration of acceptor molecules per Å<sup>3</sup> needed to quench the donor luminescence to 1/e of its value in the absence of quencher. At the critical concentration  $[A]_{\text{q}}$  there is on average exactly one acceptor molecule within the distance  $R_0$  of a donor molecule.<sup>44</sup>  $R_0$  can be determined experimentally from plots of  $\ln(I_0/I)$  versus the acceptor concentration ( $I_0$  and  $I$  are the emission intensity in absence and presence of quencher, respectively). The slope of such logarithmic plots measures  $R_0$ . This is in contrast to emission quenching in fluid solution, where it is customary to establish Stern-Volmer plots in which  $I_0/I$  is plotted against the quencher concentration; from the slope of such plots the bimolecular quenching rate constant can be calculated.<sup>45</sup>

The Perrin model can also be used for analysis of luminescence decay curves.<sup>46-51</sup> As long as the donor concentration is much lower than the acceptor concentration ( $[D] \ll [A]$ ), the donor luminescence intensity as a function of time ( $I(t)$ ) after a short excitation pulse can be expressed in the form of the tunneling radius ( $r(t)$ ) which is spanned over time  $t$ :

$$I(t)/I(t=0) = \exp[-(4/3) \cdot \pi \cdot [A] \cdot (r(t)^3 - R_0^3)] \quad (4a)$$

$$r(t) = [-3/(4 \cdot \pi \cdot [A]) \cdot \ln[I(t)/I(t=0)] + R_0^3]^{1/3} \quad (4b)$$

Equation 4b is simply a mathematical rearrangement of equation 4a. The effective tunneling radius ( $R_{\text{f}}$ ) at time  $t$  may be defined as the distance at which  $k_{\text{f}}(r) = \tau^{-1}$ .<sup>47</sup> Based on equation 1a this definition leads to equation 5, making a connection between  $R_{\text{f}}(t)$ ,  $\beta_{\text{f}}$  and  $k_{\text{f}}(R_0)$ .

$$R_f(t) = R_0 + 1/\beta_f \cdot \ln[k_f(R_0) \cdot t] \quad (5)$$

It was found that the simple Perrin model yields accurate values of  $\beta_f$  but systematically overestimates  $k_f(R_0)$  by about a factor of 2. Therefore, a revised Perrin model (equation 6a) was introduced where the factor  $g$  is simply a dimensionless constant of value 1.9.<sup>51</sup>

$$R_f(t) = R_0 + 1/\beta_f \cdot \ln[g \cdot k_f(R_0) \cdot t] \quad (6a)$$

$$= R_0 + 1/\beta_f \cdot \ln[g \cdot k_f(R_0)] + 1/\beta_f \cdot \ln(t) \quad (6b)$$

When transforming the experimental  $I(t)$ -curves into  $r(t)$ -curves using eq. 4b and plotting the resulting  $r(t)$ -values as a function of  $\ln(t)$ , one obtains linear plots that can be fitted to equation 6b; the slope of a linear regression yields  $\beta_f$ , the intercept provides  $k_f(R_0)$ .<sup>20, 52</sup> The tunneling distance  $R_f(t)$  should be independent of quencher concentration.<sup>20</sup> Consequently, luminescence decays measured at different quencher concentrations should in principle produce perfectly superimposable  $R_f(t)$ -functions; failure in doing so can reflect errors in proper intensity scaling of the different decays at  $t = 0$  (see below).<sup>19</sup> This represents a convenient (but important) self-consistency test.

Starting from the same premises as for the Perrin model (i. e., statistical distribution of D / A pairs and lack of diffusion), more sophisticated models for analysis of emission quenching in a rigid medium have been derived. One possibility is the assumption that the emissive chromophore is embedded in a face-centered cubic lattice with nearest neighbor distance  $d$ , surrounded by a random distribution of quenchers at different lattice points.<sup>18, 53, 54</sup>

$$\ln\left(\frac{I(t)}{I(t=0)}\right) = \ln(I_0(t)) - \sum_{j=1}^{\infty} \left(\frac{[Q] \cdot d^3}{2348}\right)^j \cdot \frac{1}{j} \cdot \sum_i \left[1 - \exp(-k_f(R_0) \cdot t \cdot \exp[-\beta_f \cdot (R_i - R_0)])\right] \quad (7)$$

In eq. 7, the luminescence decay relative to its value at time zero ( $I(t=0)$ ) is described as a function of the decay kinetics in the absence of quencher ( $I_0(t)$ ), the distance decay constant ( $\beta_f$ ), and the electron transfer rate constant ( $k_f(R_0)$ ) at contact distance ( $R_0$ ) between the emitter and the quencher. The factor of 2348 is appropriate for quencher concentrations measured in moles per liter and distances measured in angstroms. The sum over lattice points  $i$  excludes the origin (emitter) and any lattice points closer than  $R_0$ . The sum over  $j$  can be truncated after the first term for quencher concentrations below 5 M.<sup>53, 54</sup>

Instead of assuming that the quenchers are located at discrete lattice points one may also assume that the acceptor distribution in the rigid medium is continuous. This leads to eq. 8 which is similar to an expression derived earlier for the description of energy transfer.<sup>55</sup>

$$\ln\left(\frac{I(t)}{I(t=0)}\right) = -\frac{t}{\tau} - \frac{[A]}{132.12} \times \int_{R_0}^{\infty} \left[1 - \exp[-k_f(R_0) \cdot t \cdot \exp[-\beta_f \cdot (r - R_0)]]\right] r^2 \cdot dr \quad (8)$$

The factor of 132.12 is appropriate for quencher concentrations in units of moles per liter and distances measured in angstroms.

A rather drastic assumption made in all of these models is that reactant orientation effects do not play a significant role. This aspect has been explored in detail by Fayer,<sup>50</sup> and a comment regarding this issue is made in section 5. The models discussed above are based largely on the early work by Inokuti and Hirayama and by Hopfield;<sup>55, 56</sup> more sophisticated orientation-dependent models have been developed later.<sup>57-59</sup>

Photoinduced forward electron transfer can easily be detected by luminescence spectroscopy, but detection of the thermal backward reaction requires more sophisticated pump-probe techniques, for example transient absorption spectroscopy or transient grating experiments.<sup>60</sup> What is more, while forward electron transfer between photoexcited D and A is relatively simple to model, the problem of thermal backward electron transfer between  $D^+$  and  $A^-$  is more complex. This is because the distribution of distances between  $D^+$  and  $A^-$  is not random but instead is governed by the forward process. Since diffusion does not occur to an appreciable extent in solid matrices, back transfer is geminate, i. e., the anionic acceptor will not release its electron to a neutral donor but only to the original donor molecule which has become a cation. Due to these experimental and theoretical challenges, there exist comparatively few studies which have explored both forward and backward electron transfer between randomly dispersed donors and acceptors in rigid matrices, and the majority of case studies discussed below have focused exclusively on the photoinduced forward reaction. Nevertheless, mathematical models describing the  $D^+ / A^-$  survival probability as a function of time have been developed,<sup>16, 60-62</sup> and the results of numerical simulations are quite instructive.

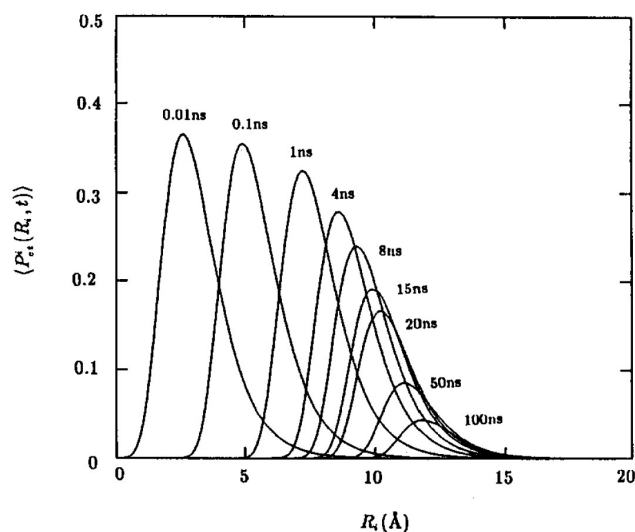


Figure 4. Most probable  $D^+ / A^-$  separation distances at various different times after pulsed excitation. The probability curves shown here were obtained with the parameters  $R_{c,f} = R_{c,b} = 10 \text{ Å}$ ,  $\beta_f = \beta_b = 1 \text{ Å}^{-1}$ ,  $\tau = 16 \text{ ns}$ , and an acceptor concentration of 0.1 M. Reprinted with permission from ref. <sup>61</sup>. Copyright 1989 American Institute of Physics.

Figure 4 shows the result of such a simulation, displaying the probability for the occurrence of a certain  $D^+ / A^-$  separation as a function of time. The simulation is based on critical quenching radii ( $R_c$ ) of 10 Å (for the forward ( $R_{c,f}$ ) and the backward ( $R_{c,b}$ ) reaction),  $\beta_f = \beta_b = 1 \text{ Å}^{-1}$ , a donor excited-state lifetime of 16 ns, and an acceptor concentration of 0.1 M.<sup>61</sup> For each time, there is

a most probable cation/anion separation, and this distance increases as time passes. The  $D^+ / A^-$  pairs which are created at early times have short separations and therefore recombine more rapidly than those generated at longer times. It has been noted that the distribution of separations moves out as a damped wave,<sup>62</sup> and the maximum separation distance is limited by the excited-state lifetime of the donor. In Figure 4 the probability curves are rather symmetrical but when  $\beta_f$  and  $\beta_b$  differ significantly, strongly asymmetric  $D^+ / A^-$  survival probabilities are calculated.<sup>62</sup>

Figure 5 was obtained using the same parameters as for Figure 4 and shows the partitioning of ion pair separations as a function of time. For example, it may be seen from this figure that (for the given set of parameters) at  $t = 10$  ns,  $D^+ / A^-$  pairs with separations shorter than 8 Å have already almost completely disappeared,  $D^+ / A^-$  pairs with a separation of 10 Å are about to reach their maximum probability, while cation-anion pairs with a separation of 15 Å are only beginning to form. The longer the  $D^+ / A^-$  separation, the slower the recombination reaction and the longer the cation-anion pair survival time. Applications of these statistical mechanics models for analysis of real experimental data will be discussed in sections 4 – 6.

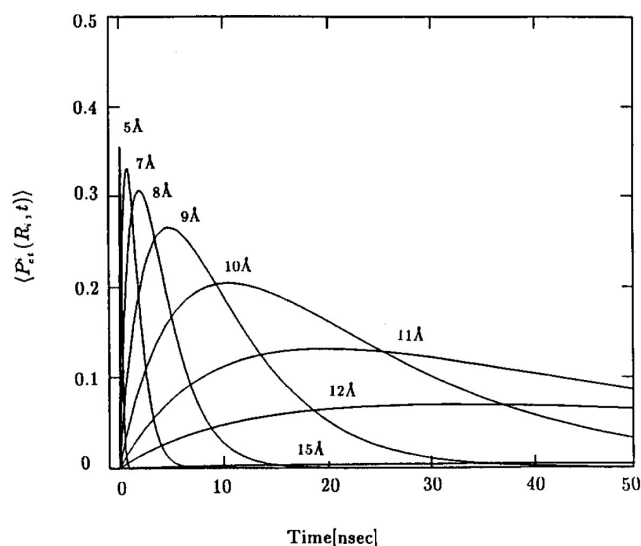


Figure 5. Probability of certain  $D^+ / A^-$  separation distances as a function of time after pulsed excitation. The curves were calculated using the same parameters as for Figure 4. Reprinted with permission from ref. <sup>61</sup>. Copyright 1989 American Institute of Physics.

In summary, the following key assumptions are usually made when analyzing data obtained from investigations of photoinduced electron transfer in glassy matrices and related rigid media: (1) donors and acceptors are dispersed in a perfectly random manner; (2) the donor-acceptor distance is fixed on the timescale of the electron transfer event; (3) the distance dependence of the electron transfer rate is dominated by the distance dependence of the electronic coupling matrix element ( $H_{DA}^2$ ) describing the electronic interaction between D and A; (4) the influence of relative D / A orientation on the electron transfer rates is neglected in most cases. When departing from an arbitrary initial pair distribution function for reactants, assumption 1 can be lifted. If the full model of electron transfer distance dependence is taken into account, assumption 3 is not

necessary.

### 3. Some practical aspects

Some of the most important practical aspects for investigation of photoinduced electron transfer between randomly dispersed donors and acceptors in rigid matrices were mentioned already in the introduction. Specifically, the most important selection criteria for donors and acceptors were outlined. Regarding the rigid matrix the key is that it can form high-quality glasses or films even when high (0.1 – 1 M) concentrations of acceptor are present. A number of pure substances and solvent mixtures form glasses when cooled to 77 K.<sup>63</sup> However, such low temperatures are not always necessary. For example, the viscosity of glycerol at 248 K is  $2.3 \cdot 10^5$  cP and hence the average diffusion distance of a glycerol molecule is  $\sim 0.5$  Å in 1  $\mu$ s (based on the Stokes-Einstein relation),<sup>64</sup> i. e., the donor-acceptor distances can be expected to remain relatively constant on the typical timescale for electron transfer with photoexcited  $Ru(\alpha\text{-diimine})_3^{2+}$  complexes. In fact higher temperatures ( $> 77$  K) may be beneficial for observing long-range electron transfer, particularly when the overall reaction requires some thermal activation.

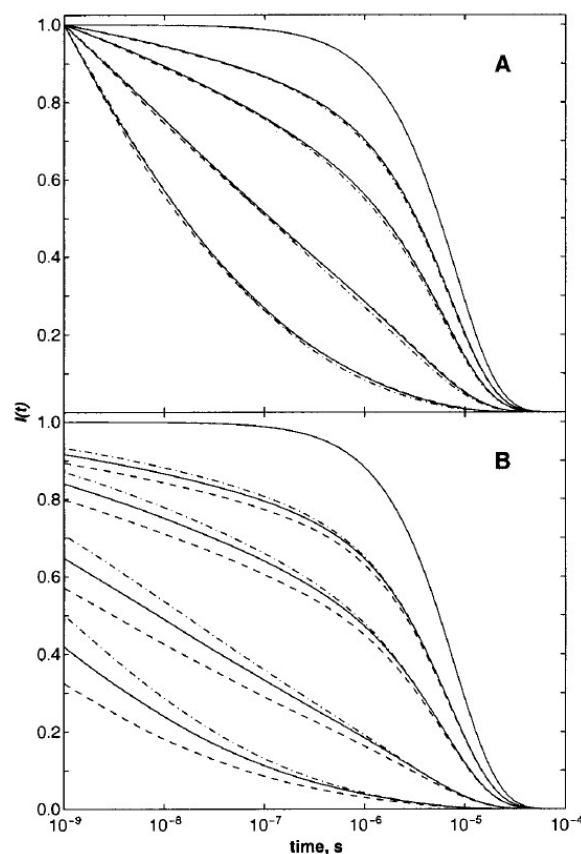


Figure 6. Simulated luminescence decay curves (using the cubic lattice model in eq. 7) for a donor – acceptor system in which the donor excited-state lifetime is 8  $\mu$ s and the acceptor concentration varies from 0 to 0.05, 0.10, 0.25, 0.50 M. For each acceptor concentration, three simulations with three different pairs of  $k_f(R_0)$  and  $\beta_f$  values were run ( $2 \cdot 10^{11} \text{ s}^{-1}$  and  $1.35 \text{ Å}^{-1}$ ;  $10^{12} \text{ s}^{-1}$  and  $1.50 \text{ Å}^{-1}$ ;  $7.5 \cdot 10^{12} \text{ s}^{-1}$  and  $1.65 \text{ Å}^{-1}$ ). In the upper panel the decay data are normalized to the earliest calculated time point (1 ns). In the lower panel the time-integrated intensities are scaled according to luminescence quantum yields. Reprinted with permission from ref. 19. Copyright 2000 American Chemical Society.

The formation of glasses at low temperatures can be associated with serious solubility issues. A homogeneous solution at 298 K does not necessarily convert into a glass of high optical quality at cryogenic temperatures even when the pure solvent is known to glass. Moreover, with increasing acceptor concentration aggregation phenomena become increasingly important, and the assumption of a statistical D / A distribution can become inappropriate. As mentioned already in the introduction, the phase change from fluid solution to rigid medium has a strong influence on  $\Delta G_{ET}^0$  and  $\lambda$ , i. e., the thermodynamics for electron transfer change significantly.<sup>26, 28</sup> As a consequence, there are numerous D / A couples which exhibit efficient excited-state electron transfer in fluid solution, but in rigid media at low temperatures the photoinduced electron transfer phenomenon cannot take place any more for thermodynamic reasons.<sup>17, 26</sup> A common strategy to circumvent this problem is to choose D / A combinations for which the driving force ( $\Delta G_{ET}^0$ ) in fluid solution is on the order of 1 eV or greater.<sup>19, 20</sup> In general, the fluid-solid phase transition also affects the photophysical properties of the emissive chromophore;<sup>28</sup> often this manifests in a lengthening of the excited-state lifetime, which is beneficial for the investigation of long-range electron transfer phenomena.

Table 1. Some rigid matrices and temperatures used for investigations of photoinduced electron tunneling between randomly dispersed donors and acceptors.

| matrix   | temperature    | references     |
|--|----------------|----------------|
| MTHF   | 77 K           | 20, 47, 48, 65 |
| triacetin-tributyrin (70:30, v/v)                              | 196 K          | 47             |
| <i>trans</i> -1,5-decalindiol                                  | 295 K          | 65             |
| ethanol  | 77 K           | 65             |
| sucrose octaacetate  | 298 K          | 50, 60, 62     |
| trehalose  | 295 K          | 66             |
| glycerol   | $\leq 250$ K   | 44, 64         |
| glycerol/methanol (9:1, v/v)                                   | 255 K          | 52, 67, 68     |
| polycarbonate "Lexan"  | 77, 298, 359 K | 49             |
| H <sub>2</sub> O with 25% (w/w) H <sub>2</sub> SO <sub>4</sub> | 77 K           | 19             |
| toluene  | 77 K           | 20             |
| mesoporous silica  | 298 K          | 69             |
| poly(ethyleneglycol)dimethacrylate                             | 298 K          | 24             |

Table 1 provides a list of host matrices that have been used for investigations of photoinduced electron tunneling between randomly dispersed donors and acceptors; the list includes highly viscous solvents, frozen glasses, and polymer films. For more extensive lists of pure substances and solvent mixtures that form frozen glasses the reader is referred to the literature.<sup>63</sup>

For the analysis of time-resolved luminescence quenching data it is very important to use decay curves which are properly scaled at  $I(t=0)$ .<sup>19, 50</sup> Figure 6 is very instructive in this regard. The upper part of Figure 6 shows a series of simulated luminescence decays for an emissive donor with an excited-state lifetime of 8  $\mu$ s and acceptor concentrations ( $[A]$ ) increasing from 0 to 0.05, 0.10, 0.25, 0.50 M.<sup>19</sup> The decay data were normalized to the earliest calculated time point (1 ns). For each of the four decays for which  $[A] \neq 0$  M three simulations with different pairs of  $k_f(R_0)$  and  $\beta_f$  values ( $2 \cdot 10^{11} \text{ s}^{-1}$  and  $1.35 \text{ \AA}^{-1}$ ;  $10^{12} \text{ s}^{-1}$  and  $1.50 \text{ \AA}^{-1}$ ;  $7.5 \cdot 10^{12} \text{ s}^{-1}$  and  $1.65 \text{ \AA}^{-1}$ ) were run. Strikingly, for any given acceptor concentration the three simulated decays obtained in this manner are nearly identical; for each concentration the three

individual simulation curves are virtually on top of each other. This shows that when experimental luminescence decay data are normalized arbitrarily,  $k_f(R_0)$  and  $\beta_f$  are strongly correlated and no unique solution can be found from fits with eq. 7. It is often difficult to determine  $I(t=0)$  directly from time-resolved experiments because the experimental setup has a limited time resolution. In these cases it becomes important to determine  $I(t=0)$  from independent measurements. The determination of relative luminescence quantum yields is a suitable way to arrive at an accurate scaling of the time-resolved data. The effect this has is nicely illustrated by the lower panel of Figure 6.<sup>19</sup> When intensities are scaled according to luminescence quantum yields, the simulations with the three different pairs of  $k_f(R_0)$  and  $\beta_f$  values from above are clearly different from each other; for each acceptor concentration one can now easily discern three different decay curves. The important message is that luminescence decay data alone are usually not sufficient for accurate determination of  $\beta$  values; complementary luminescence quantum yield measurements (relative to an unquenched sample) are usually indispensable. A recent controversy on the subject of exothermic rate restrictions in rigid media supports this statement (section 4).<sup>52, 68, 70</sup> The data self-consistency test based on eq. 6b mentioned in section 2 is highly useful in this context.<sup>20, 52</sup> Likewise, for electron transfer in fluid solution measurement of emission decay curves and time-integrated luminescence intensities is necessary in order to distinguish between static and dynamic quenching.<sup>45</sup> This issue is also very important in highly viscous solvents such as ionic liquids which are at the borderline of rigid matrices and fluid solution.<sup>21, 22</sup>

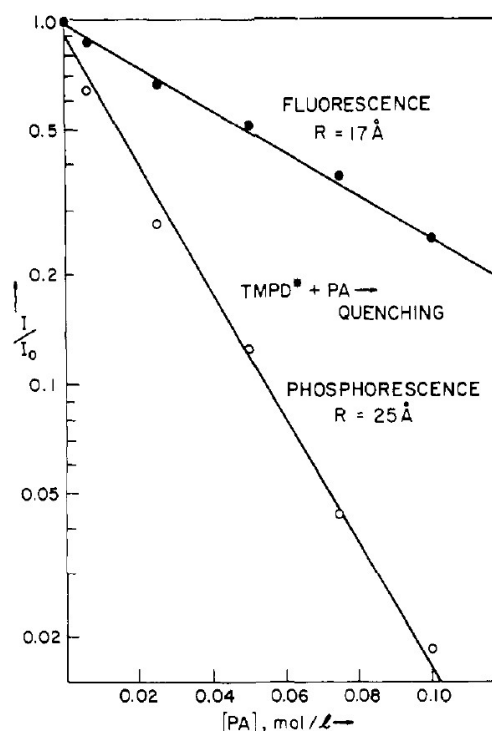


Figure 7. Decrease of fluorescence and phosphorescence intensities of photoexcited *N,N,N',N'*-tetramethyl-*p*-phenylenediamine (TMPD) as a function of phthalic anhydride (PA) concentration in a MTHF glass at 77 K. Reprinted with permission from ref. 47. Copyright 1982 American Chemical Society.

## 4. Experimental studies with organic donors and acceptors

While early studies of intermolecular electron transfer between randomly dispersed donors and acceptors in rigid matrices made use of pulse radiolysis techniques,<sup>1,9-13</sup> Miller was among the first to experimentally explore photoinduced electron tunneling in frozen glasses. Initial experiments made use of *N,N,N',N'*-tetramethyl-*p*-phenylene diamine (TMPD) as an excited-state electron donor and phthalic anhydride (PA) as an acceptor in glassy 2-methyltetrahydrofuran (MTHF) at 77 K.<sup>47</sup> The fluorescence and phosphorescence intensity (*I*) of TMPD was measured as a function of PA concentration ([PA]). Figure 7 shows a plot of *I*/*I*<sub>0</sub> versus [PA] (*I*<sub>0</sub> is the emission intensity in absence of quencher) which exhibits the expected exponential concentration dependence (section 2). Critical quenching radii (*R*<sub>c</sub>) were defined as the (center-to-center) distance at which excited-state depopulation by electron transfer is equally probable as inherent excited-state decay by fluorescence or phosphorescence. Using singlet and triplet excited-state lifetimes of 7 ns and 3 s for TMPD in MTHF at 77 K, linear regression fits to the data in Figure 7 yield *R*<sub>c</sub> = 17 Å for the fluorescent excited-state and *R*<sub>c</sub> = 25 Å for the phosphorescent excited-state of TMPD. Thus, the ~9 order of magnitude difference in lifetime between singlet and triplet excited-states only translates to an increase in electron tunneling distance by 8 Å or 47%. In the same study, three additional donors (hexaethylbenzene, hexamethyltriindan, and *N*-isopropylcarbazole) as well as two additional acceptors (pyromellitic dianhydride, tetracyanoethylene) were explored in triacetin-tributyrin (70:30, v/v) matrices at 196 K.<sup>47</sup> The largest quenching radius (*R*<sub>c</sub> = 33 Å) was determined for the phosphorescence of *N*-isopropylcarbazole with tetracyanoethylene as an acceptor.

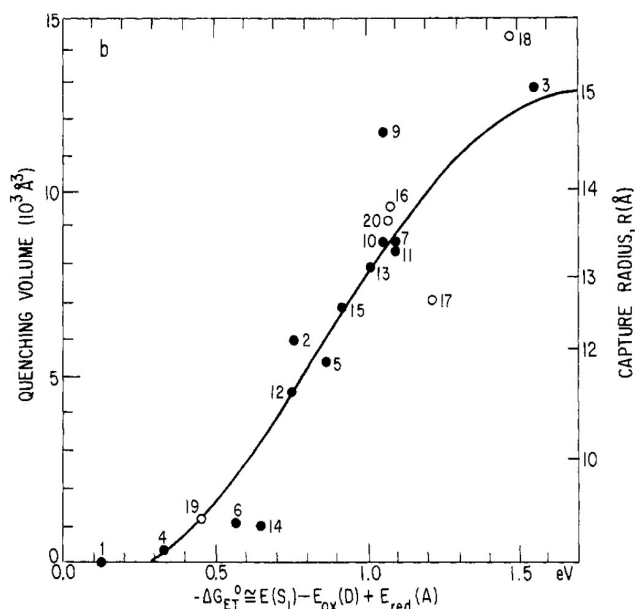


Figure 8. Gaussian free energy dependence of electron transfer rates in frozen MTHF at 77 K. Only the “normal region” is experimentally accessible. The individual data points were obtained for different donor/acceptor couples; see text for details. Reprinted with permission from ref. <sup>65</sup>. Copyright 1984 American Chemical Society.

In subsequent related work the photoexcited species was the acceptor, and various electron donors were used in large excess in a *trans*-1,5-decalindiol matrix at 295 K to induce reductive excited-state quenching by intermolecular electron transfer.<sup>65</sup> One focal point of this study was to explore the dependence of the critical quenching radius (*R*<sub>c</sub>) on the reaction free energy, hence an entire series of donor-acceptor combinations providing different electron transfer driving-forces was used. As acceptors rubrene, tetracene, 9,10-di-(2-naphtyl)anthracene, perylene, 9-methylanthracene, 9,10-diphenylanthracene, coronene, benzo[ghi]perylene, fluoranthene, and acridine were employed. TMPD, *N,N*-diethylaniline, and tetrakis(dimethylamino)ethene served as donors. Combination of these reactants permitted investigation of photoinduced electron transfer processes with reaction free energies ( $\Delta G_{ET}^0$ ) ranging from -0.1 eV to -1.5 eV (as determined for fluid polar solution). An important finding was that *R*<sub>c</sub> exhibits a Gaussian dependence on  $\Delta G_{ET}^0$  (Figure 8) as predicted by Marcus theory,<sup>30</sup> although the inverted region could not be observed in these specific experiments.<sup>65</sup> The individual excited-state acceptors have fluorescence lifetimes ranging from 0.4 ns to 380 ns, hence the critical quenching radii in Figure 8 were adjusted to the values they would have if all acceptors had an excited-state lifetime of 10 ns. The maximum quenching radius for this lifetime is 15.6 Å. For the distance decay constant ( $\beta_f$ ) a value of 1.33 Å<sup>-1</sup> was determined using the Perrin model. It was noted that the dielectric constant of the rigid *trans*-1,5-decalindiol is much lower than that of fluid acetonitrile for which the  $\Delta G_{ET}^0$  values were determined, hence the reaction free energies are most likely overestimated by 0.4 – 0.5 eV. Furthermore it was pointed out that the spherical Perrin model might be somewhat problematic for the  $\pi$ -conjugated and therefore strongly nonspherical donors and acceptors used in this study.

Subsequently, Miller and coworkers performed a closely related pulse radiolysis study in which biphenyl anion served as an electron donor, and 28 different organic molecules served as electron acceptors in vitreous MTHF at 77 K.<sup>48</sup> This technique permitted variation of  $\Delta G_{ET}^0$  over a significantly greater range (up to -2.75 eV), and in consequence made observation of the inverted driving-force effect possible. However, analysis of some of the kinetic data in the range of 10<sup>-7</sup> to 10<sup>2</sup> s turned out to be non-trivial and required the Franck-Condon factors to become time-dependent. This was justified by arguing that the solvent relaxation around the transient electron donor (biphenyl anion) is time-dependent even over very long timescales in the rigid matrix. It was noted that adjusting  $\beta_f$  would improve the fits, but a common value of  $\beta_f = 1.2$  Å<sup>-1</sup> was used to fit all data. Theoretical work suggested that such effects might have their origin in the fact that the Born-Oppenheimer approximation can become qualitatively incorrect for electron transfers at very long *D* – *A* distances.<sup>71</sup> At any rate, the distance decay constants have been demonstrated experimentally to be a function of the combination of a specific donor, acceptor, and the intervening medium.<sup>39-41</sup> Consequently, different donor-acceptor pairs in MTHF need not necessarily provide the same  $\beta_f$  value.

Fayer and coworkers used a pentacene donor, duroquinone as an acceptor, and sucrose octaacetate as a rigid matrix for investigations of photoinduced electron tunneling at room

temperature.<sup>50</sup> The key novelty of their initial study with pentacene was that for the first time the results of luminescence quenching experiments from time-resolved and time-integrated measurements were compared and found to be in excellent mutual agreement without adjustable parameters. The critical transfer distance ( $R_c$ ) defined as the distance at which an excited pentacene donor has an equal probability of decaying to the ground state as transferring an electron to a duroquinone acceptor was found to be 14.3 Å. For the distance decay parameter a value of 2.86 Å<sup>-1</sup> was determined,<sup>50</sup> suggesting that sucrose octaacetate mediates long-range electron tunneling very poorly – hardly better than what is calculated for vacuum (2.9 – 4.0 Å<sup>-1</sup>, see above).<sup>36</sup> This is a somewhat surprising result. While it is clear that individual sucrose octaacetate molecules can only interact with each other via weak van der Waals interactions, this is also true for 2-methyltetrahydrofuran molecules yet frozen glasses of this particularly solvent provide substantially lower  $\beta$ -values (see above and below).

Later work by Fayer and coworkers made use of rubrene as an electron donor in sucrose octaacetate to probe both photoinduced forward electron transfer to duroquinone acceptors, as well as thermal back electron transfer from duroquinone anions to rubrene cations.<sup>60, 62</sup> A picosecond transient grating technique was used to detect the cation/anion pairs. Data analysis was based on the sophisticated statistical mechanics models developed in the same group,<sup>50, 61</sup> and it was found that excluded volume must be taken into account in order to obtain accurate charge transfer parameters.<sup>62</sup> Briefly, the excluded volume problem arises from the fact that two molecules cannot have overlapping volumes, and at high concentrations this effect can become important and corrections to the statistical mechanics model become necessary. The critical quenching radii (defined as mentioned above) were found to be similar for the photoinduced forward reaction ( $R_{c,f}$  = 13 Å) and the thermal backward process ( $R_{c,b}$  = 13.5 Å).<sup>62</sup> For the forward reaction  $\beta_f$  = 1.25 Å<sup>-1</sup> was determined, similar to what has been found by Miller and coworkers for MTHF (1.2 Å<sup>-1</sup>) and *trans*-1,5-decalindiol (1.33 Å<sup>-1</sup>). However, analysis of the backward reaction yields  $\beta_b$  = 4.5 Å<sup>-1</sup>. The observation that forward and backward electron transfer reactions in the same intervening medium do not produce identical distance decay constants is not particularly surprising because the two reactions have different energetics and, notably, different tunneling energy gaps.<sup>34, 41, 72, 73</sup> What is surprising, however, is the very large discrepancy between  $\beta_f$  and  $\beta_b$ , and in particular the finding that the backward reaction appears to exhibit a steeper distance dependence than what has been calculated for vacuum (2.9 – 4.0 Å<sup>-1</sup>).

Eaton and coworkers investigated electron transfer from triplet-excited tryptophan to cysteine in room-temperature trehalose glasses.<sup>66</sup> Transient absorption studies yielded  $k_f(R_0)$  = 4.2·10<sup>9</sup> s<sup>-1</sup> and  $\beta_f$  = 4.0 Å<sup>-1</sup>, which is a strikingly high distance decay constant. Later measurements in aqueous glasses at 77 K have produced much lower  $\beta$  values (see below).<sup>19</sup> When  $\beta_f$  = 4.0 Å<sup>-1</sup>, only cysteines within ~1 Å of a triplet-excited tryptophan can participate in electron transfer chemistry.

## 5. Experimental studies with metal complexes

Because of efficient intersystem crossing due to large spin-orbit

coupling metal complexes usually emit from triplet excited-states which are longer-lived than the singlet excited states of purely organic molecules.<sup>74</sup> The longer the lifetime of the emissive electron donor, the longer the electron tunneling distance range that can be probed. This is the main advantage when using metal complexes, but also the fact that certain classes of metal complexes are potent excited-state donors or acceptors makes coordination compounds an interesting choice for investigating electron tunneling in rigid matrices. In initial studies by McLendon and coworkers different homo- and heteroleptic Ru( $\alpha$ -diimine)<sub>3</sub><sup>2+</sup> complexes were employed as excited-state electron donors whereas methylviologen served as an acceptor.<sup>44, 64</sup> The solid matrix was a glycerol solution which had been cooled to temperatures below 250 K; the observed exponential dependence of luminescence quenching on acceptor concentration is consistent with collisionless electron transfer (eq. 4a). Two important results emerged from these studies: (i) the distance decay constant for rigid glycerol is 1.4 Å<sup>-1</sup>, in line with prior studies in frozen MTHF by Miller ( $\beta$  = 1.2 Å<sup>-1</sup>);<sup>48</sup> (ii) the critical quenching radius ( $R_{c,f}$ ) for electron tunneling between photoexcited Ru(2,2'-bipyridine)<sub>3</sub><sup>2+</sup> and methylviologen is 13.1 Å. This corresponds to a separation of only ~3 Å between edges of the reactants hence the electron does not tunnel very far in this instance.

Subsequent studies in polycarbonate ("Lexan") made use of Ru( $\alpha$ -diimine)<sub>3</sub><sup>2+</sup> complexes as excited-state acceptors while TMPD, *N,N*-dimethyl-*p*-toluidine, *N,N*-dimethyl-*p*-methoxyaniline (PMDMA), and other amines served as electron donors.<sup>49</sup> Critical quenching radii ( $R_{c,f}$ ) in this case ranged from 8.5 to 19.3 Å, the distance decay constant was found to range between 0.50±0.07 and 0.64±0.1 Å<sup>-1</sup> depending on what ruthenium complex was used. It was cautiously considered whether this observation of donor/acceptor couple-dependent  $\beta$ -values might be related to variations in the donor/acceptor ionization potentials but the data was considered too inaccurate to permit a definite conclusion regarding this interesting question.

For biological electron transfer it is important to know how well or how badly water mediates electron tunneling. Gray and Winkler investigated photoinduced electron transfer from photoexcited Ru(terpyridine)<sub>2</sub><sup>2+</sup> to Fe(H<sub>2</sub>O)<sub>6</sub><sup>3+</sup> in aqueous glasses at 77 K, because earlier studies of electron tunneling in water did not lead to any consensus regarding the effectiveness of water as a tunneling medium.<sup>19</sup> In order to prevent crystallization, 25% (v/v) of H<sub>2</sub>SO<sub>4</sub> was added, but on a molar basis the matrix nevertheless contains >90% H<sub>2</sub>O/H<sub>3</sub>O<sup>+</sup>. Using careful steady-state and time-resolved luminescence experiments taking into account the fact that  $I(t=0)$ ,  $k_f(R_0)$ , and  $\beta_f$  are strongly interrelated (see section 3), a distance decay constant of 1.68±0.07 Å<sup>-1</sup> was determined (Figure 9). This is an important result because it demonstrates that tunneling 20 Å through water is at least 100 times slower than tunneling through protein backbone.<sup>19</sup> An electron will therefore usually prefer transferring along protein backbone over tunneling through surrounding water molecules, even at the expense of a certain geometrical detour. Mediation of electron transfer by water molecules has also been studied from a theoretical perspective.<sup>75, 76</sup>



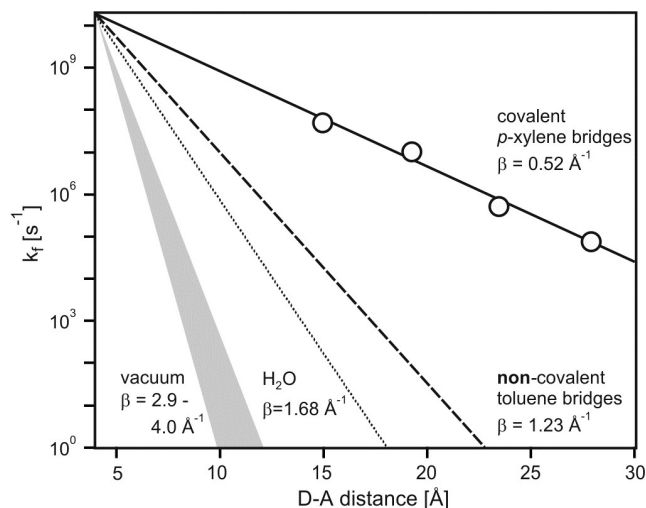


Figure 9. Timetable for electron tunneling through various media. The  $\beta$ -values for the individual tunneling media were taken from the literature.<sup>19, 20, 36, 41, 77</sup> Different donor/acceptor couples were used in the respective experiments, but here a common van der Waals contact distance of 4 Å was taken for all systems.

Subsequent studies by the Gray/Winkler team focused on the direct comparison of electron tunneling through MTHF and toluene glasses at 77 K using a dinuclear iridium complex as a donor and 2,6-dichloro-1,4-benzoquinone as the acceptor.<sup>20</sup> For MTHF  $\beta_f = 1.62 \text{ Å}^{-1}$  whereas for toluene  $\beta_f = 1.23 \text{ Å}^{-1}$  was found (Figure 9). The large distance decay constant for MTHF compared to alkane bridges ( $\beta_f = 1.0 \text{ Å}^{-1}$ )<sup>2</sup> and the higher  $\beta_f$ -value for toluene compared to covalent oligo-*p*-xylene bridges ( $\beta_f = 0.52 - 0.77 \text{ Å}^{-1}$ )<sup>20, 78, 79</sup> was attributed to the inefficiency of electron tunneling across van der Waals contacts. From these findings it was inferred that biological electron tunneling will usually occur along pathways that involve as few transfers across van der Waals contacts as possible, in line with many pathway studies of electron tunneling in proteins.<sup>20</sup> A short comment regarding reactant orientation effects seems useful here. For a D – A pair with a particular relative orientation, the electron transfer rate is, in general, orientation dependent. Fayer and coworkers demonstrated that an angle-dependent transfer rate does not have a large effect on an ensemble average observable such as a luminescence decay curve; orientation effects are simply washed out by the ensemble.<sup>50</sup> However, it has been noted that the determination of  $\beta_f$  and  $k_f(R_0)$  from an ensemble of randomly dispersed reactants could be a poor predictor for the rate of electron transfer between a donor and an acceptor held in a fixed configuration in a protein.<sup>50</sup>

Using a clever molecular design Zink and coworkers were able to determine the distance dependence of electron tunneling through mesoporous silica films.<sup>69</sup> Surfactant-templated sol-gel materials usually consist of three spatially well separated regions: (i) the silica framework, (ii) the hydrophobic core of the templating liquid crystal phase, and (iii) the ionic interface region forming the boundary between the silica framework and the hydrophobic phase. A  $\text{Ru}(\text{bpy})_3^{2+}$  complex with silylated bpy ligands was attached to the silica framework, and a methylviologen acceptor was placed into the ionic interface region. The spatial separation between the  $\text{Ru}(\text{bpy})_3^{2+}$  donor and the methylviologen acceptor thereby achieved permitted

determination of the distance dependence of electron tunneling through mesoporous silica using luminescence quenching experiments. Zink and coworkers found  $\beta_f = 2.5 \pm 0.4 \text{ Å}^{-1}$  and noted that this high value is in line with the large band gap of silica glass. This view is further in line with recent discussions of electronic conduction through an intervening medium.<sup>23</sup>

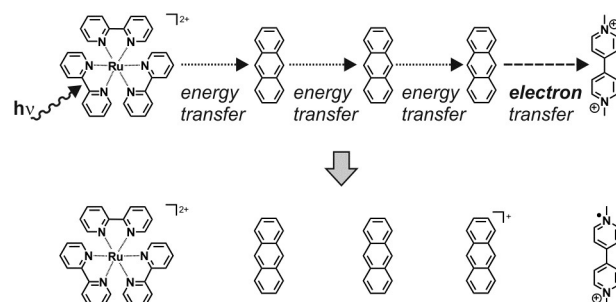


Figure 10. Illustration of the functioning principle of the sensitized ultra-long-range electron transfer process. The lower line shows the redox products which are formed after electron transfer.

## 6. Sensitized ultra-long-range electron transfer in a polymer film

In organic solar cells, photoinduced electron transfer from a donor to an acceptor-type organic semiconductor film introduces free charge carriers, i. e., donor-acceptor bilayer devices can work like classical p-n junctions.<sup>3, 5</sup> Buckminsterfullerene is a popular acceptor material for this purpose, while phenylene vinylene derivatives, polythiophene, and polyfluorene are frequently used donor-type semiconducting polymers. Blending such polymers with fullerenes is a very efficient way to break apart coulombically bound electron – hole pairs, called excitons, and to form free charge carriers. This process is called photoinduced charge separation and can occur within 50 fs in polymer blends. The charge carriers must then reach the electrodes within their lifetime.

A recent study by Meyer and coworkers makes use of the  $\text{Ru}(\text{bpy})_3^{2+}$  / methylviologen donor-acceptor couple for investigation of sensitized electron transfer through a poly(ethyleneglycol)dimethacrylate film.<sup>24</sup> This study is fundamentally different from the previously discussed studies because it involves the use of anthracene as a sensitizer of long-range electron transfer. The films contain  $\sim 50 \text{ μM}$   $\text{Ru}(\text{bpy})_3^{2+}$  donor, 0.5 mM – 9 mM methylviologen acceptor, and up to 280 mM anthracene. Following ruthenium irradiation, the excitation energy is transferred to the lowest triplet excited-state of a neighboring anthracene molecule and then migrates onwards from one anthracene unit to the next until the excitation energy is in proximity of a methylviologen dication (Figure 10). Then, methylviologen is reduced and the excited anthracene is oxidized. At methylviologen concentrations of 0.5 mM the average donor-acceptor distance was estimated to  $>90 \text{ Å}$ , i. e., the electron transfer event is sensitized through triplet-triplet energy transfer over a very long distance; for reference, tunneling distances in the works cited above were typically well below 25 Å. Given an average separation distance between anthracene molecules of 11 Å at 280 mM concentration (mathematical models for calculation of the average distance between uniformly distributed molecules are readily available),<sup>80</sup> the overall energy migration process must

involve at least 9 individual energy transfer steps. This example nicely shows how electron transfer can be sensitized by energy transfer over a very long distance in an insulating polymer.

As mentioned in section 6, there has been an investigation of photoinduced long-range electron tunneling through polycarbonate,<sup>49</sup> but given the importance of  $\pi$ -conjugated polymers for organic solar cells or OLEDs, it is surprising that there have not been many more fundamental mechanistic investigations of photoinduced electron transfer between randomly dispersed donors and acceptors in such media. There is obviously much work that has investigated the electron and hole mobility in polymer matrices by current-voltage measurements,<sup>81</sup> but this is beyond the scope of this Perspective. Likewise, investigations of photoinduced charge-separation in polymer blends (performed for example in the realm of organic solar cell or OLED research) are beyond the mission of this review on the subject of randomly dispersed donors and acceptors in rigid matrices.

## 7. Summary and conclusions

Compared to the vast amount of studies of photoinduced electron transfer in covalent donor-bridge-acceptor molecules there are relatively few studies of phototriggered electron transfer between randomly dispersed donors and acceptors in rigid matrices. Naturally the study of discrete molecules is associated with certain advantages but the covalent assembly of individual functional units is often associated with significant synthetic effort. The experimental approach discussed in this Perspective provides a valuable alternative for obtaining detailed insight into the phenomenon of long-range electron tunneling.

As mentioned already in the introduction, the field of electron tunneling in glassy matrices is rather mature but recent studies have provided some important new insights. For example, the determination of distance decay constants ( $\beta$ ) for aqueous and organic glasses using properly intensity-scaled luminescence decay data is an important result.<sup>19, 20</sup> Even though the data analysis occurred on an ensemble of D / A pairs with different relative orientations, the high  $\beta$  values of  $1.68 \pm 0.07 \text{ \AA}^{-1}$  (aqueous glass) and  $1.62 \pm 0.05 \text{ \AA}^{-1}$  (2-methyltetrahydrofuran glass) compared to protein backbone ( $\beta \approx 1.1 \text{ \AA}^{-1}$ )<sup>2, 37</sup> supports the idea that biological electron tunneling occurs largely across covalent and hydrogen-bonded pathways,<sup>75</sup> while tunneling across van der Waals contacts is avoided as much as possible. The inefficiency of electron tunneling across van der Waals contacts also manifests in a  $\beta$ -value of  $1.23 \text{ \AA}^{-1}$  for toluene glass at 77 K,<sup>20</sup> while photoinduced electron tunneling across covalently linked *p*-xylene spacers exhibits  $\beta$ -values in the range of  $0.52 \text{ \AA}^{-1}$  to  $0.77 \text{ \AA}^{-1}$  (in fluid solution at 298 K).<sup>41, 77, 78, 82-84</sup> Another important aspect that has become clear from recent investigations of electron tunneling through glasses (and from related studies with covalent donor-bridge-acceptor molecules)<sup>39, 40</sup> is that it is meaningless to report “universal” distance decay constants for a given medium; the  $\beta$ -value is always a function of the entire combination comprised of the donor, the bridging medium, and the acceptor;  $\beta$  is not a bridging medium specific constant which is universally valid for all donor-acceptor combinations.<sup>23, 39-41, 85, 86</sup>

Table 2. Some distance decay constants ( $\beta$ ) for photoinduced electron tunneling in different rigid and semirigid media.

| matrix   | $\beta [\text{\AA}^{-1}]$ | refs |
|--|---------------------------|------|
| H <sub>2</sub> O with 25% (w/w) H <sub>2</sub> SO <sub>4</sub> | $1.68 \pm 0.07$           | 19   |
| trehalose glass  | 4.0                       | 66   |
| sucrose octaacetate  | 2.86                      | 50   |
| sucrose octaacetate  | 3.33 (forward reaction)   |      |
|  | 0.83 (backward reaction)  | 60   |
| sucrose octaacetate  | 4.55 (forward reaction)   |      |
|  | 1.25 (backward reaction)  | 62   |
| glycerol   | 1.4                       | 44   |
| glycerol/methanol  | 1.65                      | 52   |
| <i>trans</i> -1,5-decalindiol                                  | 1.33                      | 65   |
| Lexan  | $0.64 \pm 0.10$           | 49   |
| 2-methyltetrahydrofuran  | 1.20                      | 48   |
| 2-methyltetrahydrofuran  | $1.62 \pm 0.05$           | 20   |
| toluene  | 1.23                      | 20   |
| mesostructured silica  | $2.5 \pm 0.4$             | 69   |

Table 2 provides a survey of distance decay constants that have been determined from studies of photoinduced electron transfer in frozen glasses and other rigid matrices. The striking observation is that these distance decay constants vary over very large ranges in identical solvents and some of them are close to the  $\beta$  value estimated for vacuum ( $2.9 - 4.0 \text{ \AA}^{-1}$ ).<sup>36</sup> For water as a tunneling medium, early pulse radiolysis studies (using aqueous glasses with 6 M NaOH) have yielded  $\beta$  values between 0.5 and  $1.4 \text{ \AA}^{-1}$ ,<sup>19, 87, 88</sup> and a transient conductance experiment in fluid solution gave  $\beta = 0.75 \text{ \AA}^{-1}$ .<sup>19, 89</sup> More recent work found  $\beta = 1.68 \pm 0.07 \text{ \AA}^{-1}$  for glassy H<sub>2</sub>O with 25% H<sub>2</sub>SO<sub>4</sub>.<sup>19</sup> It is conceivable that some of these discrepancies have their origin in the fundamentally different nature of charge-shift reactions (occurring in pulse radiolysis) and charge-separation reactions (occurring in photoinduced electron tunneling). In the latter reaction type cations and anions are formed, and the driving-force is likely to have a  $1/r$  distance dependence (as predicted from Coulomb's law). Given the low dielectric constants of the frozen media, a substantial variation in  $-\Delta G_{ET}^0$  with distance might be the result, and this could have the effect of giving larger apparent  $\beta$  values than for a comparable charge-shift reaction in the same medium. In this scenario, the resulting differences in distance decay constants are not due to variations in electronic coupling, but they are caused by the distance dependence of the driving force. This effect can potentially explain some of the variability in reported  $\beta$  values. From this discussion and the variability of the values in Table 2 it seems obvious that there is still something to understand here.

The use of properly intensity-scaled luminescence decay curves has been demonstrated recently to be of major importance for obtaining accurate  $\beta$  and  $k_f(R_0)$  values.<sup>19</sup> In early studies of photoinduced electron tunneling it is not always clear whether proper intensity-scaling of the decay curves at  $t = 0$  has been made. Consequently, it is possible that many of the  $\beta$  values obtained in the past from randomly dispersed donors and acceptors in glassy matrices are associated with very considerable error bars.

In addition to distance-dependence studies, a series of important driving-force investigations of photoinduced electron transfer in rigid media were performed only recently. In

particular, the possibility of observing the Marcus inverted region in bimolecular electron transfer has received significant attention (again),<sup>22, 52, 67</sup> despite the existence of significant earlier studies.<sup>1, 13, 65</sup> However, many of the recent observations of the inverted

region were claimed to be spurious because of inappropriate data analysis.<sup>22</sup> Proper data analysis has also been an important issue for obtaining a correct understanding of the rates for bimolecular photoinduced electron transfer in room-temperature ionic liquids.<sup>21</sup>

Given the importance of polymers for organic solar cells or OLEDs,<sup>5</sup> there have been surprisingly few fundamental (mechanistic) studies of photoinduced electron tunneling between randomly dispersed donors and acceptors in polymer matrices. Studies on polycarbonate and poly(ethyleneglycol)dimethacrylate films are notable exceptions,<sup>24, 49</sup> but analogous investigations with strongly  $\pi$ -conjugated polymers (e. g., phenylene vinylenes, polythiophenes, or polyfluorenes)<sup>3, 5</sup> in which hopping processes are expected to be more important than tunneling phenomena would be highly interesting. The plastic solar cell and OLED research communities (in which the abovementioned examples of  $\pi$ -conjugated polymers are of key importance) have mostly focussed on determining electron or hole mobilities by measuring current-voltage characteristics.<sup>3, 81</sup> Investigations of the distance dependence of photoinduced electron transfer between randomly dispersed donors and acceptors in strongly  $\pi$ -conjugated polymers have the potential to provide complementary information. To some extent, the recent study of sensitized ultra-long range electron transfer represents a step into this direction.<sup>24</sup>

In future studies, glassy matrices or polymer films could also be useful for investigations of proton-coupled electron transfer (PCET) reactions. The dependence of the overall PCET rate on the electron transfer distance is yet poorly understood (contrary to “simple” electron transfer not involving proton motion). Recent investigations in this context focused on donor-bridge-acceptor molecules that have to be made in laborious multi-step syntheses.<sup>90-93</sup>

## Acknowledgments

The author thanks Jay R. Winkler (Caltech) for valuable discussions. Several anonymous reviewers are thanked for valuable comments.

## Notes and references

<sup>a</sup> Universität Basel, Departement Chemie, Spitalstrasse 51, CH-4056 Basel, Switzerland. Fax: +41 (0)61 267 09 76; Tel: +41 (0)61 267 11 46; E-mail: oliver.wenger@unibas.ch

- 1 R. G. Compton, *Electron Tunneling in Chemistry*, Elsevier, Amsterdam, New York, 1989.
- 2 H. B. Gray and J. R. Winkler, *Proc. Natl. Acad. Sci. U. S. A.*, 2005, **102**, 3534.
- 3 S. Günes, H. Neugebauer and N. S. Sariciftci, *Chem. Rev.*, 2007, **107**, 1324.
- 4 G. Gustafsson, Y. Cao, G. M. Treacy, F. Klavetter, N. Colaneri and A. J. Heeger, *Nature*, 1992, **357**, 477.
- 5 A. J. Heeger, *Rev. Mod. Phys.*, 2001, **73**, 681.
- 6 D. Rehm and A. Weller, *Isr. J. Chem.*, 1970, **8**, 259.
- 7 L. T. Calcaterra, G. L. Closs and J. R. Miller, *J. Am. Chem. Soc.*, 1983, **105**, 670.
- 8 L. S. Fox, M. Kozik, J. R. Winkler and H. B. Gray, *Science*, 1990, **247**, 1069.
- 9 J. R. Miller, *Chem. Phys. Lett.*, 1973, **22**, 180.
- 10 J. R. Miller, *Science*, 1975, **189**, 221.
- 11 J. R. Miller and J. V. Beitz, *J. Chem. Phys.*, 1981, **74**, 6746.
- 12 A. Kira, *J. Phys. Chem.*, 1981, **85**, 3047.
- 13 J. V. Beitz and J. R. Miller, *J. Chem. Phys.*, 1979, **71**, 4579.
- 14 M. Tachiya and A. Barzykin, *Chem. Phys.*, 2005, **319**, 222.
- 15 R. A. Marcus, *J. Phys. Chem.*, 1990, **94**, 4963.
- 16 M. Tachiya and A. Mozumder, *Chem. Phys. Lett.*, 1975, **34**, 77.
- 17 K. V. Mikkelsen and M. A. Ratner, *Chem. Rev.*, 1987, **87**, 113.
- 18 M. Tachiya and A. Mozumder, *Chem. Phys. Lett.*, 1974, **28**, 87.
- 19 A. Ponce, H. B. Gray and J. R. Winkler, *J. Am. Chem. Soc.*, 2000, **122**, 8187.
- 20 O. S. Wenger, B. S. Leigh, R. M. Villahermosa, H. B. Gray and J. R. Winkler, *Science*, 2005, **307**, 99.
- 21 M. Koch, A. Rosspeintner, G. Angulo and E. Vauthey, *J. Am. Chem. Soc.*, 2012, **134**, 3729.
- 22 A. Rosspeintner, M. Koch, G. Angulo and E. Vauthey, *J. Am. Chem. Soc.*, 2012, **134**, 11396.
- 23 P. P. Edwards, H. B. Gray, M. T. J. Lodge and R. J. P. Williams, *Angew. Chem. Int. Ed.*, 2008, **47**, 6758.
- 24 A. Ito, D. J. Stewart, Z. Fang, M. K. Brennaman and T. J. Meyer, *Proc. Natl. Acad. Sci. U. S. A.*, 2012, **109**, 15132.
- 25 A. J. Heeger, *Chem. Soc. Rev.*, 2010, **39**, 2354.
- 26 G. L. Gaines, M. P. Oneil, W. A. Svec, M. P. Niemczyk and M. R. Wasielewski, *J. Am. Chem. Soc.*, 1991, **113**, 719.
- 27 W. E. Jones, P. Y. Chen and T. J. Meyer, *J. Am. Chem. Soc.*, 1992, **114**, 387.
- 28 P. Y. Chen and T. J. Meyer, *Chem. Rev.*, 1998, **98**, 1439.
- 29 O. S. Wenger, H. B. Gray and J. R. Winkler, *Chimia*, 2005, **59**, 94.
- 30 R. A. Marcus and N. Sutin, *Biochim. Biophys. Acta*, 1985, **811**, 265.
- 31 D. Segal, A. Nitzan, W. B. Davis, M. R. Wasielewski and M. A. Ratner, *J. Phys. Chem. B*, 2000, **104**, 3817.
- 32 S. S. Isied, A. Vassilian, J. F. Wishart, C. Creutz, H. A. Schwarz and N. Sutin, *J. Am. Chem. Soc.*, 1988, **110**, 635.
- 33 B. S. Brunschwig, S. Ehrenson and N. Sutin, *J. Am. Chem. Soc.*, 1984, **106**, 6858.
- 34 H. M. McConnell, *J. Chem. Phys.*, 1961, **35**, 508.
- 35 M. Tachiya and S. Murata, *J. Phys. Chem.*, 1992, **96**, 8441.
- 36 J. N. Onuchic, D. N. Beratan, J. R. Winkler and H. B. Gray, *Annu. Rev. Biophys. Biomol. Struct.*, 1992, **21**, 349.
- 37 H. B. Gray and J. R. Winkler, *Ann. Rev. Biochem.*, 1996, **65**, 537.
- 38 F. Giacalone, J. L. Segura, N. Martín and D. M. Guldi, *J. Am. Chem. Soc.*, 2004, **126**, 5340.
- 39 M. P. Eng and B. Albinsson, *Chem. Phys.*, 2009, **357**, 132.
- 40 B. Albinsson, M. P. Eng, K. Pettersson and M. U. Winters, *Phys. Chem. Chem. Phys.*, 2007, **9**, 5847.
- 41 O. S. Wenger, *Acc. Chem. Res.*, 2011, **44**, 25.
- 42 B. C. Dahlen and D. R. Tyler, *Macromolecules*, 2008, **41**, 9525.
- 43 R. C. Dorfman, M. Tachiya and M. D. Fayer, *Chem. Phys. Lett.*, 1991, **179**, 152.
- 44 S. Strauch, G. McLendon, M. McGuire and T. Guarr, *J. Phys. Chem.*, 1983, **87**, 3579.
- 45 O. Stern and M. Volmer, *Phys. Z.*, 1919, **20**, 183.
- 46 F. Perrin, *Compt. Rend.*, 1924, **178**, 1978.
- 47 J. R. Miller, K. W. Hartman and S. Abrash, *J. Am. Chem. Soc.*, 1982, **104**, 4296.
- 48 J. R. Miller, J. V. Beitz and R. K. Huddleston, *J. Am. Chem. Soc.*, 1984, **106**, 5057.
- 49 T. Guarr, M. E. McGuire and G. McLendon, *J. Am. Chem. Soc.*, 1985, **107**, 5104.
- 50 R. P. Domingue and M. D. Fayer, *J. Chem. Phys.*, 1985, **83**, 2242.
- 51 R. K. Huddleston and J. R. Miller, *J. Phys. Chem.*, 1982, **86**, 200.
- 52 P. J. S. Gomes, C. Serpa, R. M. D. Nunes, L. G. Arnaut and S. J. Formosinho, *J. Phys. Chem. A*, 2010, **114**, 2778.
- 53 A. Blumen, *J. Chem. Phys.*, 1980, **72**, 2632.
- 54 A. Blumen and J. Manz, *J. Chem. Phys.*, 1979, **71**, 4694.
- 55 M. Inokuti and F. Hirayama, *J. Chem. Phys.*, 1965, **43**, 1978.
- 56 D. G. Thomas, J. J. Hopfield and W. M. Augustyniak, *Phys. Rev.*, 1965, **140**, A202.
- 57 A. A. Demidenko and E. G. Petrov, *Teor. Eksp. Khimiya*, 1989, **25**, 222.

- 58 A. B. Doktorov, R. F. Khairutdinov and K. I. Zamaraev, *Chem. Phys.*, 1981, **61**, 351.
- 59 K. I. Zamaraev and R. F. Khairutdinov, *Chem. Phys.*, 1974, **4**, 181.
- 60 R. C. Dorfman, Y. Lin, M. B. Zimmt, J. Baumann, R. P. Domingue and M. D. Fayer, *J. Phys. Chem.*, 1988, **92**, 4258.
- 61 Y. Lin, R. C. Dorfman and M. D. Fayer, *J. Chem. Phys.*, 1989, **90**, 159.
- 62 R. C. Dorfman, Y. Lin and M. D. Fayer, *J. Phys. Chem.*, 1989, **93**, 6388.
- 63 R. S. Drago, *Physical Methods for Chemists*, Reinhold Publishing Company, New York, 1965.
- 64 T. Guarr, M. McGuire, S. Strauch and G. McLendon, *J. Am. Chem. Soc.*, 1983, **105**, 616.
- 65 J. R. Miller, J. A. Peeples, M. J. Schmitt and G. L. Closs, *J. Am. Chem. Soc.*, 1982, **104**, 6488.
- 66 L. J. Lapidus, W. A. Eaton and J. Hofrichter, *Phys. Rev. Lett.*, 2001, **87**.
- 67 P. J. S. Gomes, C. Serpa, R. M. D. Nunes, L. G. Arnaut and S. J. Formosinho, *J. Phys. Chem. A*, 2010, **114**, 10759.
- 68 C. Serpa, R. M. D. Nunes, L. G. Arnaut and S. J. Formosinho, *J. Phys. Chem. A*, 2011, **115**, 7861.
- 69 E. Johansson and J. I. Zink, *J. Am. Chem. Soc.*, 2007, **129**, 14437.
- 70 G. Angulo, A. Rosspeintner and E. Vauthey, *J. Phys. Chem. A*, 2011, **115**, 7858.
- 71 D. N. Beratan and J. J. Hopfield, *J. Chem. Phys.*, 1984, **81**, 5753.
- 72 K. Pettersson, J. Wiberg, T. Ljungdahl, J. Mårtensson and B. Albinsson, *J. Phys. Chem. A*, 2006, **110**, 319.
- 73 J. Wiberg, L. J. Guo, K. Pettersson, D. Nilsson, T. Ljungdahl, J. Mårtensson and B. Albinsson, *J. Am. Chem. Soc.*, 2007, **129**, 155.
- 74 A. Ito and T. J. Meyer, *Phys. Chem. Chem. Phys.*, 2012, **14**, 13731.
- 75 J. P. Lin, I. A. Balabin and D. N. Beratan, *Science*, 2005, **310**, 1311.
- 76 N. E. Miller, M. C. Wander and R. J. Cave, *J. Phys. Chem. A*, 1999, **103**, 1084.
- 77 D. Hanss and O. S. Wenger, *Inorg. Chem.*, 2008, **47**, 9081.
- 78 D. Hanss, M. E. Walther and O. S. Wenger, *Coord. Chem. Rev.*, 2010, **254**, 2584.
- 79 O. S. Wenger, *Chem. Soc. Rev.*, 2011, **40**, 3538.
- 80 S. Chandrasekhar, *Rev. Mod. Phys.*, 1943, **15**, 0001.
- 81 A. C. Arias, J. D. MacKenzie, I. McCulloch, J. Rivnay and A. Salleo, *Chem. Rev.*, 2010, **110**, 3.
- 82 D. Hanss and O. S. Wenger, *Inorg. Chem.*, 2009, **48**, 671.
- 83 D. Hanss and O. S. Wenger, *Eur. J. Inorg. Chem.*, 2009, 3778.
- 84 M. E. Walther, J. Grilj, D. Hanss, E. Vauthey and O. S. Wenger, *Eur. J. Inorg. Chem.*, 2010, 4843.
- 85 O. S. Wenger, *Inorg. Chim. Acta*, 2011, **374**, 3.
- 86 J. Hankache and O. S. Wenger, *Phys. Chem. Chem. Phys.*, 2012, **14**, 2685.
- 87 J. R. Miller, *J. Phys. Chem.*, 1975, **79**, 1070.
- 88 I. V. Alexandrov, R. F. Khairutdinov and K. I. Zamarev, *Chem. Phys.*, 1978, **32**, 123.
- 89 K. H. Schmidt, P. Han and D. M. Bartels, *J. Phys. Chem.*, 1995, **99**, 10530.
- 90 M. Kuss-Petermann, H. Wolf, D. Stalke and O. S. Wenger, *J. Am. Chem. Soc.*, 2012, **134**, 12844.
- 91 J. J. Warren, A. R. Menzeleev, J. S. Kretchmer, T. F. Miller, H. B. Gray and J. M. Mayer, *J. Phys. Chem. Lett.*, 2013, **4**, 519.
- 92 O. S. Wenger, *Acc. Chem. Res.*, 2013, doi: 10.1021/ar300289x.
- 93 O. S. Wenger, *Chem.-Eur. J.*, 2011, **17**, 11692.

60